FPGA-based smart camera for accurate chlorophyll estimations

Madain Perez-Patricio, Abiel Aguilar-González, Jorge L Camas-Anzueto,
Nestor Antonio Morales Navarro, Rubén R Grajales-Coutiño

FPGA-based smart camera for accurate chlorophyll estimations

5 authors, including:

Madain Perez-Patricio
Instituto Tecnológico de Tuxtla Gutiérrez
24 PUBLICATIONS   **65** CITATIONS

SEE PROFILE

Abiel Aguilar-González
Instituto Nacional de Astrofísica, Óptica y Electrónica (INAOE)
20 PUBLICATIONS   **37** CITATIONS

SEE PROFILE

Jorge luisc camas anzueto
Instituto Tecnológico de Tuxtla Gutiérrez
53 PUBLICATIONS   **177** CITATIONS

SEE PROFILE

Some of the authors of this publication are also working on these related projects:

Project   mechatronics devices for aerial images acquisition View project

Project   Processing natural language View project

FPGA-based smart camera for accurate chlorophyll estimations

Madaín Pérez-Patricio*[1] | Abiel Aguilar-González[2,3] | J. L. Camas-Anzueto[1] | N. Morales-Navarro[1] | R. Grajales-Coutiño[1]

[1]Mechatronics Engineering Department, Instituto Tecnológico de Tuxtla Gutiérrez (ITTG), Chiapas, Mexico
[2]Computer Science Department, Instituto Nacional de Astrofísica, Óptica y Electrónica (INAOE), Puebla, Mexico
[3]Institut Pascal, Université Clermont Auvergne (UCA), Auvergne, France

Correspondence
*Madaín Pérez-Patricio, Carretera Panamericana Km. 1080, C.P. 29050, Apartado Postal: 599. Email: mperez@ittg.edu.mx

Summary

In this work, a new chlorophyll estimation approach based on the reflectance/transmittance from the leaf being analyzed is proposed. First, top/underside images from the leaf under analysis are captured, then, the base parameters (reflectance/transmittance) are extracted. Finally, a double-variable linear regression model estimates the chlorophyll content. In order to estimate the base parameters, a novel optical arrangement is presented. On the other hand, in order to provide a portable device, suitable for chlorophyll estimation under large scale food crops, we have implemented our optical arrangement and our algorithmic formulation inside an FPGA-based smart camera fabric. Experimental results demonstrated that the proposed approach outperforms (in terms of accuracy and processing speed) most previous vision-based approaches, reaching more than 97% accuracy and delivering fast chlorophyll estimations (near 5ms per estimation).

KEYWORDS:
Chlorophyll estimation, smart camera, FPGA

1 | INTRODUCTION

Smart cameras are image/video acquisition devices with self-contained image processing algorithms that simplify the formulation of a particular application [1,2]. For example, algorithms for smart video surveillance could detect and track pedestrians [3], but for a robotic application, algorithms could be feature detection or feature tracking [4,5]. In this work, the aim is for a fast/accurate solution for the chlorophyll estimation problem. This is motivated because previous work has limitations due to high processing time and cost or low accuracy. In general, laboratory tests deliver high accuracy (ground truth) but processing time and cost are high. In practice, others techniques, faster and cheaper than laboratory tests are used, unfortunately, in most cases these techniques have low accuracy or the system size makes it difficult to implement under large scale food crops. In our case, we believe that a smart camera that addresses the chlorophyll estimation problem could be a useful contribution for the current state of the art since fast estimations with compact system design could be obtained.

1.1 | Chlorophyll estimation under food crops

Given the current population growth rate, food crops demand has been highly increased. So, in order to obtain more efficient crops, most of the current food producers supervise their crops health since it is well known that stress conditions affect photosynthetic activity. In recent years, one popular approach consists in estimate the chlorophyll content in the plants leaves within a crop [6,7,8,9,10,11,12,8]. This is because there is a high correlation between the chlorophyll content and the plants health [13] then,

in current literature, several approaches for chlorophyll estimation can be found [14,15]. In most cases, devices such as the Soil Plant Analysis Development (SPAD) are used for the chlorophyll estimation [16,17]. In general, the SPAD device measures the leaf absorbance at several wavelengths. Then, based on the absorbance, a SPAD numerical value, proportional with the chlorophyll content, is computed. In theory the SPAD device delivers fast estimations with high accuracy. Unfortunately, in practice it only estimates the absorbance at one point of the leaf under analysis. i.e., it estimates the chlorophyll content within a small spatial location of the leaf. To solve this problem, it is necessary to make iterative measurements at different spatial locations. Finally, the average value corresponds with the chlorophyll content, in addition, the high cost of the SPAD technology makes it difficult to implement under large scale food crops. Other trend, that aims for low cost and fast chlorophyll estimations, are vision-based approaches [12,8]. In this context, image processing algorithms are applied with the assumption that chlorophyll content defines the leaf color. i.e., low chlorophyll contents generate yellowish-green colors while high chlorophyll content involves dark green colors. In previous works, several vision based approaches have been proposed and several image processing algorithms have been developed [6,7,8,9,10,11], unfortunately, it was demonstrated that they achieve relatively low accuracy (compared with the SPAD device).

1.2 | Motivation and scope

In this work, the aim is for a fast/accurate solution for the chlorophyll estimation problem, in addition, we are interested in a compact system design since this could be useful under large food crops in which portable devices are desirables. The contribution of this work is twofold, first, this work proposes a novel mathematical formulation that uses the reflectance/transmittance within the visible electromagnetic spectrum range as base parameters for the chlorophyll estimation. Second, an FPGA-based smart camera capable to capture the base parameters (reflectance/transmittance) and where the chlorophyll estimation is carried out in a parallel architecture is presented. The rest of this manuscript is organized as follows: **Section** 2 presents the related work. In **Section** 3, details about the proposed approach, details about the FPGA architecture and our smart camera implementation are shown. Experimental results and comparison with previous works are detailed in **section** 4. Finally, **Section** 5 concludes this manuscript.

2 | RELATED WORK

Approaches such as [12,8] capture images with airborne cameras. These techniques have the advantage of monitoring large land areas. Unfortunately, their cost is high (higher than the SPAD-based approach) and there is no control for ambient lighting changes that decreases the accuracy. There are other approaches that capture images at different wavelengths. In particular, multispectral and hyperspectral images with 300 - 1200 nm have been used [6,7,8,9,10,11]. Other authors [18,19,20,21] have used images with visible spectrum (300-700 nm) information in order to determine a correlation value between chlorophyll/nitrogen content. In general, multispectral/hyperspectral based approaches reach relatively high accuracy and real time processing. Unfortunately, their cost and size are high (similar size than the SPAD device and similar cost but with lower accuracy). Other approach, that could be more efficient in terms of system design and cost, could be the use of a single RGB (Red-Green-Blue color space) camera. In previous work there exist some research for nitrogen and calcium estimations. In [22], RGB images from four plants groups, each group with a different nitrogen level (0%, 50%, 100%, and 150% of the required daily dose) were captured at 5 different growth states (10, 20, 30, 40, and 50 days). Plant leaves were placed on a white surface. Then, an RGB-based classifier estimates the nitrogen content as deficient or in excess. In [23] two color space are used in order to detect calcium deficiency in lettuce plants. Values as color, entropy, energy, contrast, and homogeneity were used as health indicators. Then, calcium deficiency is computed via statistical computations. In both cases [22] and [23] the use of a single RGB camera allowed for a compact system design and low cost but accuracy is low.

3 | MATERIALS AND METHODS

In this section details about the proposed approach are presented. It consists of a novel optical arrangement that captures the proposed base parameters (reflectance/transmittance). Then, an image processing algorithm extracts the base parameters. Finally, a double-variable linear regression model estimates the chlorophyll content.

3.1 | Dataset

In this work, more than 400 plants with different health states were tested. For that, several hydroponic crops (Lactuca sativa) were cultivated. In these crops, different nutritional solutions were applied in order to obtain different health levels for the plants within the crop. So, 27 nutritional solutions with different macronutrients concentrations were prepared. Each nutritional solution, corresponds to 0%, 50% or 100% of the daily nutritional requirements. Each nutritional solution was applied for three different plants within the crop and this process was replicated for 6 different crops. Finally, one SPAD device was used to measure the SPAD values that corresponds with the chlorophyll content, all measures were realized after 15 grown days, where the plants have reach maturity and there are not symptoms of damages due to the age. Using this chlorophyll values we could estimate our crop health, however, to determine crop health is a complex task since it depends on several factors: the crop type, plantation procedures, weather are important issues. Even the geographical location or any type of external agent such as dust or snow can affect the health. For example, given a particular crop, chlorophyll values equal to 41 could represent a high health level in some world regions but in other regions a good chlorophyll values could be 37. In practice, the food producers determine their crops health given their particular conditions. For this reason, in this work we will only focus on the chlorophyll estimation, that is the basis of the crop health estimations.

3.2 | The base parameters

Previous work demonstrated that there are two crucial issues in the chlorophyll estimation procedures. The first one is for the acquisition technique using to capture the base parameters. In general, all acquisition techniques are sensitive to noise and this decreases the accuracy. The second issue is for the base parameters using for the chlorophyll estimation. Robust base parameters should deliver accurate results. Nevertheless, previous vision-based approaches demonstrated that it is difficult to obtain base parameters with high discriminant and repeatability [1][24]. For the acquisition technique, previous vision-based approaches have used natural illumination and this has delivered poor performance in terms of accuracy. In this work we believe that one alternative to this problem could be using light sources with known frequency. Then, more controlled environment, could deliver more accurate measurements. For the base parameters, previous work demonstrated that chlorophyll content is close related with the color components in the leaf being analyzed [25,26]. In this work, we propose the color reflectance/transmittance in the leaf being analyzed as base parameters since we believe that these parameters deliver high discriminant and robustness, higher than the base parameters used in previous works.

3.3 | The proposed smart camera

In order to capture the base parameters, a novel optical arrangement inside our smart camera fabric is proposed, see **Fig. 1** . In general, one CCD imager connected in a TRDB DC2 development board is used to provide a 1280×1024 Bayer pattern image where the images are acquired in RGB format. The imager provides raw format with 10 bits per pixel. The external specifications are: 5.8 × 4.92 mm, and the lens used has 8 mm focal length. The imager was placed at 39° opposed to horizontal inclination (in order to observe simultaneously the upper/lower part of the leaf), and 100 mm of vertical distance. The viewing angle is computed using **Eq.** 1; where α is the vertical or horizontal viewing angle, s the vertical or horizontal dimension and f the focal distance. Considering the visual field perpendicular to the viewing angle bisector, then, it has to full encompass the glass and the mirror. So, the bisector d (**Fig. 1** a) represents the necessary distance between the vision field and the imager, and it is computed by **Eq.** 2; where d is the bisector and l the visual field longitude. Finally, the imager is focused on the optical arrangement visual field line and the diaphragm opening is adjusted to $f = f/8$. For the light source, one MCWHD2 LED (800 mW) is used. In addition, the optical arrangement uses a 50×70 millimeter glass that support the leaf being analyzed and, at the bottom, a 70 mm square mirror which reflects the leaf transmittance information. Pieces of black matte plastic control the light flow within the device and reduce the entry of outside light.

$$\alpha = 2tan^{-1}\frac{s}{2f} \tag{1}$$

---

[1]Discriminant: for different chlorophyll values, different base parameters responses have to be obtained. In practice, low discriminant values decrease the performance since several chlorophyll values (within a small range) could have similar base parameters response. Repeatability: for similar chlorophyll values, similar base parameters responses have to be obtained. In some cases, this affirmation is not true and different leafs (with similar chlorophyll content) deliver different base parameters responses.

$$d = \frac{l}{2tan\frac{\alpha}{2}} \tag{2}$$

3.4 | Image processing

In **Fig.** 2 a), one example of the images captured by our optical arrangement is shown. Then, given the upper part of **Fig.** 2 a) contain the reflectance information ($I_1(x, y)$) and the lower part contain the transmittance ($I_2(x, y)$), the proposed algorithm computes the reflectance (R_r) and transmittance (T_r) as shown in **Eq.** 3-4; where $I_1(x, y, r, c)$ are the red channel pixel values for c different samples taken from ($I_1(x, y)$) and $I_2(x, y, r, c)$ are the red channel pixel values for c different samples from ($I_2(x, y)$), see **Fig.** 2 b), in this example 8 different samples were extracted. Finally, **Eq.** 5 estimates the chlorophyll content, it was obtained using linear regression, more details can be found in the following section.

$$R_r = \frac{\sum_1^c I_1(x, y, r, c)}{c} \tag{3}$$

$$T_r = \frac{\sum_1^c I_2(x, y, r, c)}{c}, \tag{4}$$

$$F(R_r, T_r) = 42.44 + 0.4043R_r - 0.7541T_r \tag{5}$$

3.5 | The base parameters performance

Table 1 presents average values for transmittance/reflectance and their respective chlorophyll content in SPAD values, where $R\{R, G, B\}, T\{R, G, B\}$ are the values for reflectance/transmittance for each RGB channel. In **Fig.** 3 the reflectance/transmittance values, in relation with the SPAD values are shown. From **Fig.** 3 a), in all channels reflectance increases as the amount of chlorophyll increases. This is because high chlorophyll content absorbs high light energy. On the other hand, **Fig.** 3 b) shows that higher chlorophyll content reduces the transmittance value for all the channels. This is because high chlorophyll content reduces the light that passes through the leaf.

3.6 | The linear regression model

In order to build a chlorophyll estimation framework, any statistical regression model have to fulfil with the linear dependence between chlorophyll values and the base parameters. In our case, linear regression is used due to its mathematical simplicity that involves high processing speed with low computational requirements. It was tested with different combinations of the base parameters proposed in this work. It was demonstrated that all the proposed parameters deliver high accuracy and in particular, the combination of both, provide accuracy superior to most previous vision-based approaches (similar than SPAD measurements). In **Table** 2 , results of applying single-variable linear regression models for each values presented in **Table** 1 are shown. The maximum $R2 = 94.51$ is for the red channel transmittance $F(Tr)$, the smallest standard deviation $SD = 1.19$ and the best mean absolute error $MAE = 1.01$ is also for $F(Tr)$. Thus, it is demonstrated that the best variable to estimate the chlorophyll content is the transmittance in red channel. In **Table** 3 , results of applying double-variable linear regression models for each values presented in **Table** 1 are shown. The best $R2 = 97.73.59$ is for the combination of reflectance and transmittance in the red channel $F(R_r, T_r)$, in addition, this combination has the best standard deviation $SD = 0.72$. and the best mean absolute error $MEA = 0.60$. So, it is demonstrated that the combination of reflectance and transmittance in the red channel $F(R_r, T_r)$ deliver the best performance for chlorophyll estimation.

3.7 | The FPGA architecture

In **Fig.** 4 , the developed FPGA architecture is shown. In general, the CCD sensor deliver raw images with 10 bpp as stream, P[29:0]. Key[3:0] is used for the camera control. Then, the FPGA architecture extracts c samples from the input image, see **Eq.** 3-4. Finally, the chlorophyll content is computed according **Eq.** 5 where the · operation is implemented using a look-up table

(LUT), R_r and T_r are the index values and, the output value which represents the chlorophyll content is selected using also a LUT.

3.7.1 | The image acquisition module

One CCD imager connected in a TRDB DC2 developement board is used as keystone of the image acquisition module. It provides 1280×1024 RGB images with 10 bits per pixel. In order to reduce hardware requirements, only the most significant 8 bits of the data provided by the TRDB DC2 board are used.

3.7.2 | The sampling module

In **Fig.** 5 the FPGA architecture of the sampling module is shown. The P[23:0], Hcont[10:0] and Vcont[11:0] are the data input for the sampling module (the x, y spatial location form the image pixels). Both: (Hcont[10:0] and Vcont[10:0]) are compared with defined values that corresponds with the spatial coordinates of the sample pixels that corresponds with the transmittance/reflectance areas. Then, each retained value are saved into logical registers.

3.8 | The chlorophyll estimation module

Fig. 6 shows the chlorophyll estimation module. This module applies **Eq.** 5. The mean for the sample values are computed add all the values and taking the eight most significant values. In **Tables** 4 and 5 the LUTs used in this step are shown.

4 | RESULTS

The developed FPGA architecture was implemented in an FPGA Cyclone II EP2C35F672C6 of Altera. All modules were designed via Quartus II Web Edition version 10.1SP1. All modules were validated via post-synthesis simulations performed in ModelSim Altera and, in **Table** 6 the hardware resource consumption for the developed FPGA architecture is shown. It is demonstrated that the regression model $F(R_r, T_r)$ delivers a robust framework for chlorophyll estimation. $R2 = 97.73$, mean absolute error $MAE = 0.60$ and standard deviation $SD = 0.72$ are reached, see **Table** 3 .

In **Table** 7 , accuracy comparisons with respect to previous vision-based approaches are shown. In our case, we compared the proposed algorithm given different sampling values. It was demonstrated that sample values between 8-32 to deliver high accuracy and robustness for the chlorophyll estimation process. On the other hand, the proposed approach outperform all previous vision based approaches. This is because previous formulations use base parameters that have low stability under illumination changes. For this work, due to the wide availability of RGB cameras with low cost, the proposed solution could be a promising chlorophyll estimation framework, similar accuracy and size than SPAD but lower cost and lower processing time (near 5 ms per estimation). For processing speed, in all cases, the proposed algorithm reaches real-time processing (faster than SPAD measurements and previous vision-based approaches). For the system size in all cases, our smart camera, see **Fig.** 7 uses a small FPGA device as processor, in addition all the optical/image acquisition components are inside the camera fabric.

5 | CONCLUSIONS

In this work, a novel chlorophyll estimation approach was proposed. First, we have proposed a new mathematical formulation that uses color reflectance/transmittance from the leaf being analyzed as base parameters for chlorophyll estimation. Second, we have developed a new FPGA-based smart camera, capable to capture the base parameters and where all the algorithmic part is processed in a parallel architecture. It was demonstrated that reflectance/transmittance deliver robust/discriminant values for chlorophyll estimations. Experimental results demonstrated that a double-variable linear regression learning algorithm achieves 97% accuracy under a Lactuca sativa hydroponic crop. In addition, the proposed approach delivers fast measurements with low cost and allow compact system design (similar than the SPAD device). In this work, the proposed algorithm was applied on a Lactuca sativa crop. In order to determine if other crop types present similar patterns, the mathematical model could be expanded to several different food crops. In any case, the smart camera layout and the formulation of the learning algorithm have to be the same. Only color comparison of the crop being analyzed and some minor adjustments in the multiple regression model would be needed.

References

1. Carey Stephen J, Barr David RW, Dudek Piotr. Low power high-performance smart camera system based on SCAMP vision sensor. *Journal of Systems Architecture.* 2013;59(10):889–899.

2. Bourrasset Cédric, Maggianiy Luca, Sérot Jocelyn, Berry François, Pagano Paolo. Distributed FPGA-based smart camera architecture for computer vision applications. In: :1–2IEEE; 2013.

3. Hengstler Stephan, Prashanth Daniel, Fong Sufen, Aghajan Hamid. MeshEye: a hybrid-resolution smart camera mote for applications in distributed intelligent surveillance. In: :360–369ACM; 2007.

4. Aguilar-González Abiel, Arias-Estrada Miguel, Berry François. Dense Feature Matching Core for FPGA-based Smart Cameras. In: :41–48; 2017.

5. Aguilar-González Abiel, Arias-Estrada Miguel, Berry François. Robust feature extraction algorithm suitable for real-time embedded applications. *Journal of Real-Time Image Processing.* 2017;:1–19.

6. Noh H, Zhang Q. Shadow effect on multi-spectral image for detection of nitrogen deficiency in corn. *Computers and electronics in agriculture.* 2012;83:52–57.

7. Zhang Xiaolei, Liu Fei, He Yong, Gong Xiangyang. Detecting macronutrients content and distribution in oilseed rape leaves based on hyperspectral imaging. *Biosystems engineering.* 2013;115(1):56–65.

8. Delegido Jesús, Van Wittenberghe Shari, Verrelst Jochem, et al. Chlorophyll content mapping of urban vegetation in the city of Valencia based on the hyperspectral NAOC index. *Ecological Indicators.* 2014;40:34–42.

9. Huang Min, Wan Xiangmei, Zhang Min, Zhu Qibing. Detection of insect-damaged vegetable soybeans using hyperspectral transmittance image. *Journal of Food Engineering.* 2013;116(1):45–49.

10. Diezma Belén, Lleó Lourdes, Roger Jean Michel, Herrero-Langreo Ana, Lunadei Loredana, Ruiz-Altisent Margarita. Examination of the quality of spinach leaves using hyperspectral imaging. *Postharvest Biology and Technology.* 2013;85:8–17.

11. Navarro-Cerrillo Rafael Mᵃ, Trujillo Jesus, Orden Manuel Sánchez, Hernández-Clemente Rocío. Hyperspectral and multispectral satellite sensors for mapping chlorophyll content in a Mediterranean Pinus sylvestris L. plantation. *International Journal of Applied Earth Observation and Geoinformation.* 2014;26:88–96.

12. Saberioon MM, Amin MSM, Anuar AR, Gholizadeh A, Wayayok A, Khairunniza-Bejo Siti. Assessment of rice leaf chlorophyll content using visible bands at different growth stages at both the leaf and canopy scale. *International Journal of Applied Earth Observation and Geoinformation.* 2014;32:35–45.

13. Officer Protection. Food and agriculture organization of the United Nations. 2016;.

14. Wan Wenbo, Hua Dengxin, Le Jing, He Tingyao, Yan Zhe, Zhou Chunyan. Study of laser-induced chlorophyll fluorescence lifetime measurement and its correction. *Measurement.* 2015;60:64–70.

15. Fernandez-Jaramillo Arturo Alfonso, Jesus Romero-Troncoso Rene, Duarte-Galvan Carlos, et al. FPGA-based chlorophyll fluorescence measurement system with arbitrary light stimulation waveform using direct digital synthesis. *Measurement.* 2015;75:12–22.

16. Muñoz-Huerta Rafael F, Guevara-Gonzalez Ramon G, Contreras-Medina Luis M, Torres-Pacheco Irineo, Prado-Olivarez Juan, Ocampo-Velazquez Rosalia V. A review of methods for sensing the nitrogen status in plants: advantages, disadvantages and recent advances. *Sensors.* 2013;13(8):10823–10843.

17. Hu Hao, Zhang Guangzhi, Zheng Kefeng. Modeling leaf image, Chlorophyll fluorescence, reflectance from SPAD readings. *IEEE Journal of Selected Topics in Applied Earth Observations and Remote Sensing.* 2014;7(11):4368–4373.

18. Fernández-Pacheco Daniel G, Escarabajal-Henarejos David, Ruiz-Canales Antonio, Conesa Julián, Molina-Martínez Jose M. A digital image-processing-based method for determining the crop coefficient of lettuce crops in the southeast of Spain. *Biosystems engineering.* 2014;117:23–34.

19. Wiwart Marian, Fordoński Gabriel, Żuk-Gołaszewska Krystyna, Suchowilska Elżbieta. Early diagnostics of macronutrient deficiencies in three legume species by color image analysis. *Computers and electronics in agriculture.* 2009;65(1):125–132.

20. Juan Wang, Changzhou Wei, Jinqiang Guo, Yongwen Lei. A method based on digital image analysis for estimating crop canopy parameters. In: :7–10IEEE; 2011.

21. Wang Yuan, Wang Dejian, Zhang Gang, Wang Jun. Estimating nitrogen status of rice using the image segmentation of GR thresholding method. *Field Crops Research.* 2013;149:33–39.

22. Ma Lili, Fang Junlong, Chen Yuehua, Gong Shuipeng. Color Analysis of leaf images of deficiencies and excess nitrogen content in soybean leaves. In: :1–3IEEE; 2010.

23. Story David, Kacira Murat, Kubota Chieri, Akoglu Ali, An Lingling. Lettuce calcium deficiency detection with machine vision computed plant features in controlled environments. *Computers and Electronics in Agriculture.* 2010;74(2):238–243.

24. Dey Amar Kumar, Sharma Manisha, Meshram MR. An Analysis of Leaf Chlorophyll Measurement Method Using Chlorophyll Meter and Image Processing Technique. *Procedia Computer Science.* 2016;85:286–292.

25. Hu Hao, Zhang Jizong, Sun Xiangyang, Zhang Xiaoming. Estimation of leaf chlorophyll content of rice using image color analysis. *Canadian Journal of Remote Sensing.* 2013;39(2):185–190.

26. Tewari VK, Arudra Ashok Kumar, Kumar Satya Prakash, Pandey Vishal, Chandel Narendra Singh. Estimation of plant nitrogen content using digital image processing. *Agricultural Engineering International: CIGR Journal.* 2013;15(2):78–86.

27. Pagola Miguel, Ortiz Rubén, Irigoyen Ignacio, et al. New method to assess barley nitrogen nutrition status based on image colour analysis: comparison with SPAD-502. *Computers and electronics in agriculture.* 2009;65(2):213–218.

28. Moghaddam Parviz Ahmadi, Derafshi Mohammadali Haddad, Shirzad Vine. Estimation of single leaf chlorophyll content in sugar beet using machine vision. *Turkish Journal of Agriculture and Forestry.* 2011;35(6):563–568.

29. Kawashima Shigeto, Nakatani Makoto. An algorithm for estimating chlorophyll content in leaves using a video camera. *Annals of Botany.* 1998;81(1):49–54.

TABLE 1 Reflectance and transmittance values

SPAD value (C)	Reflectance			Transmittance		
	RR	RG	RB	TR	TG	TB
27.52	47.408	54.26	36.361	46.117	50.384	28.293
28.3	46.481	53.905	35.26	44.683	49.458	27.027
28.94	45.814	52.921	34.782	43.887	48.514	26.601
29.09	41.948	49.597	34.338	39.806	45.42	24.403
29.16	41.718	46.58	34.456	38.992	42.99	23.965
30.17	42.392	50.156	34.992	37.703	42.585	23.586
31.22	40.619	48.52	32.928	35.066	40.792	21.564
31.41	41.777	47.296	32.518	35.439	39.162	21.089
32.62	43.12	49.835	34.141	35.574	40.44	21.213
34.00	40.159	50.379	31.667	32.41	40.885	19.585
34.23	42.299	49.604	31.913	33.268	40.147	19.578
35.36	42.924	55.595	32.071	33.411	40.377	19.378
35.47	43.252	49.98	33.499	32.449	35.014	20.154
35.82	44.173	50.337	32.611	32.545	34.864	19.389
36.38	47.116	51.16	32.699	33.028	34.468	19.356
37.98	37.167	46.722	30.45	26.015	31.265	17.72
39.68	38.78	46.485	30.114	26.306	30.673	17.334
39.88	37.623	47.76	30.999	25.484	31.136	16.852
40.31	37.543	40.051	28.256	23.067	24.265	14.492
40.66	38.086	39.974	28.522	22.704	23.955	13.304
41.67	43.2455	44.697	31.88	23.027	24.216	14.377

TABLE 2 Regression Models (single-variable)

Independent Variables	R2(%)	Standard deviation (SD)	Mean absolute error (MAE)
F (Rr)	90.22	1.6976	3.0232
F (Rg)	90.67	2.6	2.92
F (Rb)	88.52	2.27	1.73
F (Tr)	94.51	1.19	1.01
F (Tg)	93.65	1.35	1.03
F (Tb)	93.24	1.3	1.11

TABLE 3 Regression Models (double-variable)

Independent Variables	R2(%)	Standard deviation (SD)	Mean absolute error (MAE)
F (Rr, Tr)	97.73	0.72	0.60
F (Rg, Tg)	97.11	0.77	0.67
F (Rb, Tb)	97.27	0.79	0.61
F (Rr, Tg)	97.71	0.76	0.72
F (Rg, Tb)	94.47	1.12	0.92
F (Rb, Tr)	92.63	1.17	1.04
F (Rr, Tb)	95.72	0.97	0.81
F (Rg, Tr)	95.43	0.86	0.79
F (Rb, Tg)	96.11	0.77	0.89

TABLE 4 Look up table for the linear regresion

R_r	$R_r \times 0.4043$	T_r	$T_r \times -0.7542$
50	20	50	-38
49	20	49	-37
48	19	48	-36
47	19	47	-35
46	18	46	-35
45	18	45	-34
44	17	44	-33
43	17	43	-32
42	17	42	-32
41	16	41	-31
40	16	40	-30
39	15	39	-29
38	15	38	-29
37	15	37	-28
36	14	36	-27
35	14	35	-26
34	13	34	-26
33	13	33	-25
32	13	32	-24
31	12	31	-23
30	12	30	-23

TABLE 5 Look up table for the chlorophyll estimation

$F(R_r, T_r)$	SPAD/chlorophyll value
-18	24
-17	25
-16	26
-15	27
-14	28
-13	29
-12	30
-11	31
-10	32
-9	33
-8	34
-7	35
-6	36
-5	37
-4	38
-3	39
-2	40
-1	41
0	42

TABLE 6 Hardware resource consumption for the developed FPGA architecture

Resource	Demand
Total logic elements	1535 (7%)
Total pins	154 (100%)
Total memory bits	64,856 (11%)
Total PLLs	2 (50%)

TABLE 7 Vision based approaches for chlorophyll estimation: accuracy

Approach	Accuracy (%)
H. Noh and Q. Zhang (2012)[6], Whole area	86
H. Noh and Q. Zhang (2012)[6], Bright area	87
H. Noh and Q. Zhang (2012)[6], Corn area	85
Tewari et.al (2013)[26]	93.8
Hao Hu et. al (2014)[17], Green Value	74
Hao Hu et. al (2014)[17], Red Value	74.7
Pagola et. al (2009)[27], IpcaM4	91.89
Pagola et. al (2009)[27], IpcaM2	92.24
Moghaddam et.al (2011)[28], MLPN	94
Moghaddam et.al (2011)[28], R, B (regression)	88
Kawashima et al. (1998)[29], NORMALISED 'r'	79
Kawashima et al. (1998)[29], NORMALISED 'g'	76
This work,$F(R_r, T_r)$, $n = 4$	92.54
This work,$F(R_r, T_r)$, $n = 8$	97.73
This work,$F(R_r, T_r)$, $n = 16$	97.81
This work,$F(R_r, T_r)$, $n = 32$	97.79

(a) 2D diagram (b) 3D diagram
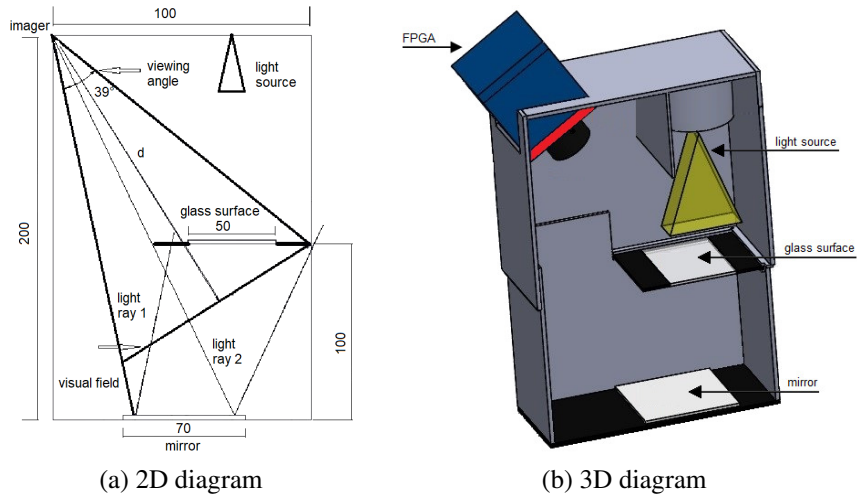
FIGURE 1 The proposed smart camera: the leaves were inserted in the smart camera and the optical arrangement extracts the base parameters, then, the imager shots the leaves and finally, an FPGA architecture estimates the chlorophyll content.
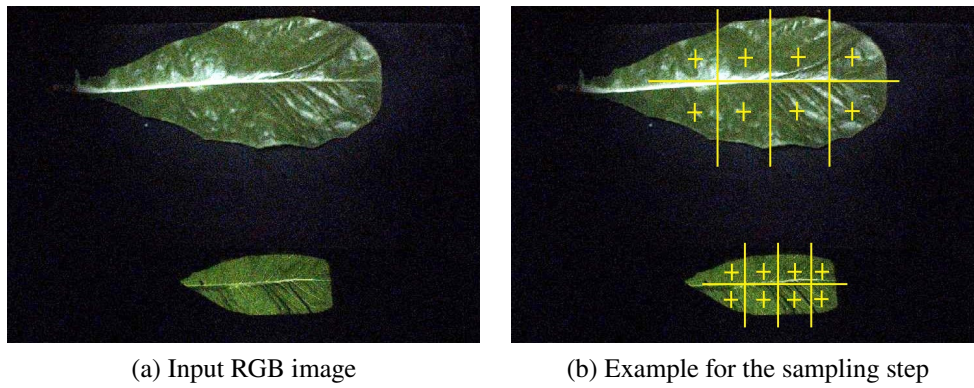

(a) Input RGB image (b) Example for the sampling step

FIGURE 2 The image processing step. Given an RGB image from the leaf being analyzed, several pixel values which corresponds with the reflectance/transmittance are extracted.

(a) Chlorophyll vs reflectance

(b) Chlorophyll vs transmitance
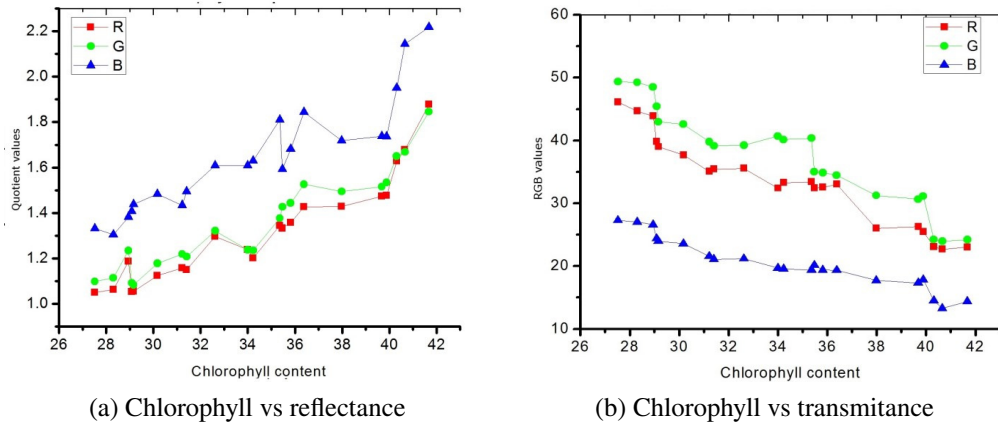
FIGURE 3 The base parameters performance. Experimental results demonstrate that the reflectance value increases as the amount of chlorophyll increases. On the other hand, higher chlorophyll content reduces the transmittance value.
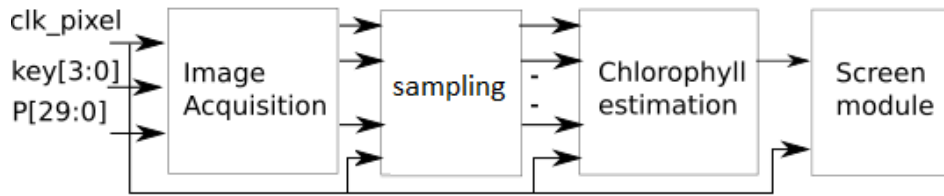

FIGURE 4 General diagram of the developed FPGA architecture. First, one CCD sensor deliver raw images with 10 bpp as stream (P[29:0]. Key[3:0]) is used for the camera control. Then, the FPGA architecture extracts c samples from the input image. Then, the chlorophyll content is computed using a look-up table. Finally, results are displayed to the user in a screen.
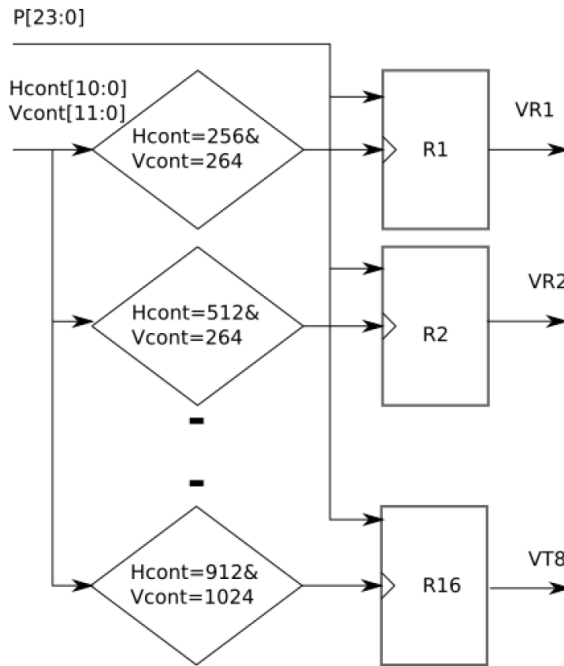

FIGURE 5 FPGA architecture for the sampling module. Given the x,y spatial location form the image pixels, then the x,y values are compared with predefinded spatial values wich corresponds with the spatial coordinates of the sample pixels. These samples corresponds with the transmittance/reflectance areas and are saved into logical registers.
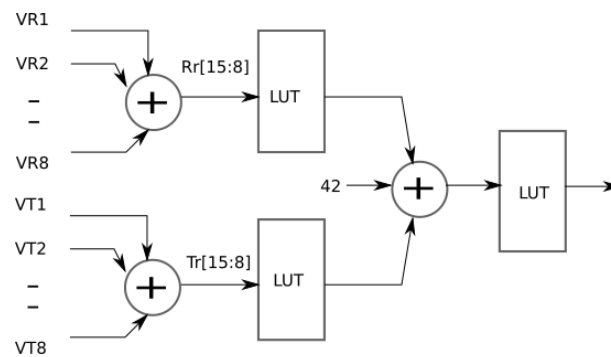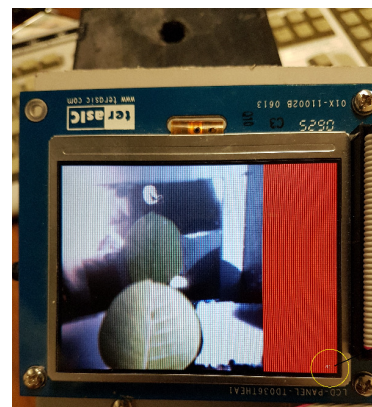
FIGURE 6 FPGA architecture for the chlorophyll estimation module. First, the mean for the sample values are computed adding all the sample values and taking the eight most significant values. Then the chlorophyll content is estimated using a look-up table.

(a) Acquisition process

(b) Results

FIGURE 7 The developed smart camera. One CCD imager connected in a TRDB DC2 development board is used to provide a 1280×1024 Bayer pattern image. The optical arrangement uses a 50×70 millimeter glass that support the leaf being analyzed and, at the bottom, a 70 mm square mirror which reflects the leaf transmittance information. Pieces of black matte plastic control the light flow within the device and reduce the entry of outside light.